

Application of Lai and Juang Methods for Liquefaction Probability Analysis in Petobo, Palu

Penerapan Metode Lai dan Juang untuk Analisis Probabilitas Likuiifikasi di Petobo, Palu

Nia Dwi Ariyanti¹, Galuh Chrismaningwang^{2*}, Yusep Muslih Purwanai³, Raden Harya Dananjaya⁴

^{1,2,3,4} Department of Civil Engineering-Faculty of Engineering-Sebelas Maret University, Surakarta, Indonesia
Correspondence address: Ir. Sutami Street No. 36, Kentingan, Jebres, Surakarta, Central Java, Indonesia 57126
email: galuh@ft.uns.ac.id*

Abstract

Liquefaction is a phenomenon where the soil loses its strength and rigidity, rendering it unable to support structures, often triggered by seismic activity. In Petobo, Palu City, a 7,4 magnitude earthquake caused significant subsidence and casualties, underscoring the area's susceptibility to liquefaction. This study investigates the liquefaction potential in Petobo using N-SPT data and evaluates the probability of liquefaction based on Factor of Safety (FS) values. The analysis employs probabilistic methods by Lai et al. (2006) and Juang et al. (2008), using an empirical approach based on FS. Results from six test points (LP-1 to LP-6) reveal that liquefaction potential exists at LP-2, LP-4, and LP-5, with varying risks influenced by the earthquake's magnitude. LP-5 demonstrates a high liquefaction potential, with a Liquefaction Potential Index (LPI) between 4 and 15 across different seismic magnitudes. Additionally, LP-5 shows a high probability of liquefaction, with the Lai method indicating "Almost Certainly Liquefied" at 0,99, while the Juang method suggests "Not Likely to Liquefy" at 0,32. The findings highlight that higher earthquake magnitudes significantly increase LPI values and liquefaction probabilities, emphasizing the importance of seismic considerations in the region.

Keywords: Petobo; Earthquake; Liquefaction; DEEPSOIL; Probability_Method

Abstrak

Likuiifikasi adalah fenomena di mana tanah kehilangan kekuatan dan kekakuannya, sehingga tidak mampu menopang struktur, yang sering kali dipicu oleh aktivitas seismik. Di Petobo, Kota Palu, gempa berkekuatan 7,4 SR menyebabkan penurunan permukaan tanah yang signifikan dan jatuhnya korban jiwa, menggarisbawahi kerentanan daerah tersebut terhadap likuiifikasi. Studi ini menyelidiki potensi likuiifikasi di Petobo dengan menggunakan data N-SPT dan mengevaluasi probabilitas likuiifikasi berdasarkan nilai Factor of Safety (FS). Analisis ini menggunakan metode probabilistik oleh Lai dkk. (2006) dan Juang dkk. (2008), dengan menggunakan pendekatan empiris berdasarkan FS. Hasil dari enam titik uji (LP-1 hingga LP-6) menunjukkan bahwa potensi likuiifikasi ada di LP-2, LP-4, dan LP-5, dengan risiko yang berbeda-beda yang dipengaruhi oleh magnitudo gempa. LP-5 menunjukkan potensi likuiifikasi yang tinggi, dengan Indeks Potensi Likuiifikasi (LPI) antara 4 hingga 15 pada magnitudo gempa yang berbeda. Selain itu, LP-5 menunjukkan probabilitas likuiifikasi yang tinggi, dengan metode Lai menunjukkan "Hampir Pasti Likuiifikasi" sebesar 0,99, sedangkan metode Juang menunjukkan "Tidak Mungkin Likuiifikasi" sebesar 0,32. Temuan ini menyoroti bahwa magnitudo gempa yang lebih tinggi secara signifikan meningkatkan nilai LPI dan probabilitas likuiifikasi, yang menekankan pentingnya pertimbangan seismik di wilayah tersebut.

Kata Kunci: Petobo; Gempa Bumi; Likuiifikasi; DEEPSOIL; Metode_Probabilitas

Please cite this article as:

Ariyanti, N. D., Chrismaningwang, G., Purwanai, Y. M., & Dananjaya, R. H. (2024). Application of Lai and Juang Methods for Liquefaction Probability Analysis in Petobo, Palu. *Media Teknik Sipil*, 22(2), 39-50. <https://doi.org/10.22219/jmts.v22i2.35768>

INTRODUCTION

An earthquake is a natural phenomenon when the ground surface shakes due to the sudden release of energy when rocks in the Earth's layers crack or shift. Indonesia is one of the countries highly prone to natural disasters, particularly earthquakes. This condition arises because Indonesia is located at the convergence of three tectonic plates: the Pacific, Indo-Australian, and Eurasian. Additionally, Indonesia lies on the active volcanic belt known as the 'Pacific Ring of Fire' (Fuady et al., 2021).

Geographically, Palu City is located in an active earthquake zone. Palu City has a high risk of earthquakes, caused by the activity of Palu Koro (Leopatty et al., 2022). In addition, the Central Sulawesi region, including Palu City and Donggala Regency, has a very high earthquake potential. One of the impacts caused by earthquakes is liquefaction. This condition can trigger various events such as quick settlement, tilting of building foundations, differential settlement, and wells where water dries up and is replaced by non-cohesive material.

Liquefaction occurs when granular solid materials transform into a liquid state due to increased pore water pressure and decreased effective stress (Tijow et al., 2018). In analysing the liquefaction potential, it is essential to investigate the magnitude of the factor of safety (FS) and the probability of liquefaction (P_L).

This research uses the DEEPSOIL application to analyse the earthquake in Palu by obtaining the a_{max} value, which is crucial in analyzing liquefaction probability. The liquefaction probability analysis in this study uses the methods proposed by (Lai et al., 2006) and (Juang et al., 2008) with data based on FS values. This probability analysis is conducted to determine the size, location, and frequency of earthquakes in the Petobo area of Palu. This study is expected to help strengthen the assumption that there is a potential for liquefaction in a particular area.

Various studies related to liquefaction probability analysis have been conducted. This research continues the research conducted by (Pamungkas, 2023), which analysed the potential for liquefaction using the Simplification and LPI methods. The results of the previous research analysis

assessed whether liquefaction potential could occur based on the safety factor (FS). Unlike prior studies, this study analyses the probability of liquefaction developed by Lai et al. (2006) and Juang et al. (2008). This method provides an overview of how much liquefaction potential may occur.

Rahman (2020), analysed liquefaction in the Yogyakarta International Airport (NYIA) Underpass Area by using SPT data and applying the liquefaction Potential Index (LPI) method (Rahman et al., 2020).

Mase (2018), analysed the probability of liquefaction in coastal Bengkulu City based on the 8.4 Mw earthquake that occurred on September 12, 2007, using SPT data and several best-fit methods, namely Seed, Tokimatsu & Yoshimi, JRA (Japan Rail Association), Youd & Idriss, and Idriss & Boulanger methods (Mase, 2018). In addition, this study also used several methods for liquefaction probability analysis based on FS values, such as Hwang et al. (2004), Somnez and Gokceoglu (2005), Lai et al. (2006), and Juang et al. (2008).

Based on the above research, liquefaction probability analysis is very important to study, as it can predict the worst-case likelihood of liquefaction occurring at a location due to an earthquake or other ground movements. Similarly, studies on using the DEEPSOIL application to analyse earthquake data in liquefaction probability analysis still need to be completed.

The application of DEEPSOIL for analyzing earthquake data in liquefaction probability analysis is an area that requires further exploration. Current studies have utilized various methodologies, including deterministic and probabilistic approaches, to assess liquefaction potential, but the integration of DEEPSOIL remains under-researched.

Deterministic and Probabilistic Approaches: Research has shown that both approaches can effectively assess liquefaction potential, with studies using SPT data to calculate factors of safety and liquefaction indices (Poddar et al., 2023).

Machine Learning Models: Recent advancements include machine learning techniques, such as RNN and CNN, which have demonstrated superior predictive capabilities for liquefaction potential based on extensive datasets (Kumar et al., 2023).

soil layers with an FC value $\leq 35\%$, or FC $> 35\%$ with an IP value ≤ 15 ; and soil layers with $d_{50} \leq 10\%$ and $d_{10} \leq 1\%$.

Second, the earthquake was analysed using the DEEPSOIL application, which provides output from a_{max} values for calculating the Cyclic Stress Ratio (CSR). This program can perform one-dimensional seismic site response analysis nonlinearly and linearly and produces output in graphs and tables (Hashash, 2024). The analysis can begin with selecting the type of analysis to be used. Next, input the soil parameters, including the thickness of soil layers, soil density, shear wave velocity, and soil shear strength.

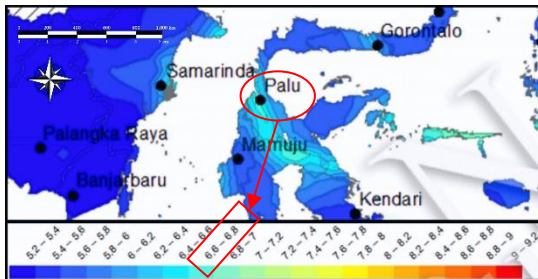


Figure 3. Magnitude (M) of Palu on the Deaggregation Map for a 2500-year return period (2022, n.d.)

Then, ground motions were selected by conducting a disaggregation analysis using the Indonesian Earthquake Hazard Deaggregation Map for Planning and Evaluation of Earthquake Resistant Infrastructure in 2022, as presented in Figures 3 and 4. This analysis provides results in magnitude values, distances, and corresponding earthquake source mechanisms.

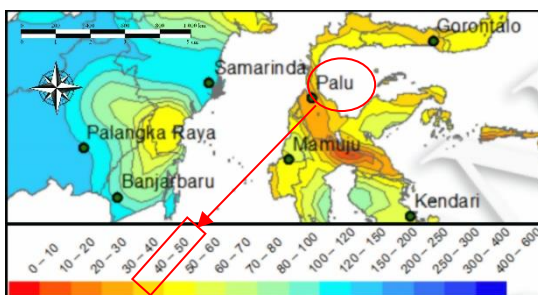


Figure 4. Distance (R) of Palu on the Deaggregation Map for a 2500-year return period (2022, n.d.)

Based on the results of the disaggregation analysis, magnitude (M) and distance (R) parameters are obtained. These parameters are

used to determine the accelerogram that will be used as ground motion input. The accelerogram can be obtained from PEER (Pacific Earthquake Engineering Research) data through the website <https://ngawest2.berkeley.edu>.

The accelerograms obtained through the PEER website must undergo a scaling process before being used as input motion in the ground response analysis. The scaling process aims to obtain artificial accelerograms suitable for the review conditions. The scaling process was carried out using the DEEPSOIL application.

The final step in the DEEPSOIL analysis is to set the necessary parameters and options for the analysis process, including configuring the type of analysis, desired outputs, and other relevant settings.

Third, the liquefaction potential will be analysed using the simplification method. In this method, the Cyclic Stress Ratio (CSR) and Cyclic Resistance Ratio (CRR) values are used to obtain the safety factor (FS) value. In this study, the CSR value can be calculated from Equation 1.

$$CSR = \frac{\tau_{av}}{\sigma'_{vo}} = 0,65 \left(\frac{a_{max}}{g} \right) \left(\frac{\sigma_{vo}}{\sigma'_{vo}} \right) r_d \quad [1]$$

Where a_{max} : peak seismic acceleration (PGA), g : acceleration of gravity, σ_{vo} : total vertical overburden stress (kN/m^2), σ'_{vo} : effective vertical overburden stress (kN/m^2), and r_d : reduction stress coefficient.

Then, the CRR value for magnitudes other than Mw 7,5 can be calculated using Equation 2, proposed by (Youd & Idriss, 2001), as follows.

$$CRR_{Mw} = CRR_{7,5} \times MSF \times K_{\sigma} \times K_{\alpha} \quad [2]$$

Where CRR_{Mw} : CRR for earthquakes with magnitudes other than 7,5, MSF: magnitude scale factor, K_{σ} : influential stress correction factor, and K_{α} : slope correction factor. The values of K_{σ} and K_{α} are generally calculated for specific conditions; therefore, in this study, the values of K_{σ} and K_{α} are 1.

After determining the CSR and CRR values, the next step is to compare the values to get the factor of safety (FS) value using the following equation.

$$FS = \frac{CRR_{Mw}}{CSR} \quad [3]$$

Fourth, the liquefaction probability is analysed to predict how much liquefaction potential occurs. This analysis uses the probability method developed by Lai et al. (1996) and Juang et al. (2008) based on the FS values obtained from the liquefaction analysis. Liquefaction probability analysis is calculated by applying Equation [4] for Lai's method and Equation [5] for Juang's method.

$$P_L = \frac{1}{1+0,2(FS)^3+0,8(FS)^7} \quad [4]$$

$$P_L = \frac{1}{\left(1 + \frac{FS}{1,06}\right)^{3,8}} \quad [5]$$

Table 1. Liquefaction classes based on liquefaction probability (Chen & Juang, 2000)

Class	Probability	Description
5	$P_L > 0,85$	Almost certainly liquefied
4	$0,65 < P_L \leq 0,85$	Very likely to liquefy
3	$0,35 < P_L \leq 0,65$	Possible
2	$0,15 < P_L \leq 0,35$	Not likely to be liquefied
1	$P_L \leq 0,15$	Almost certainly not liquefied

The probability values for liquefaction potential result in the liquefaction probability (P_L) for future cases. Table 1, proposed by Chen and Juang (2000), interprets the liquefaction probability calculations.

Fifth, analyze the Liquefaction Potential Index (LPI) to measure the severity of liquefaction impact by considering the influence of FS and the depth weighting factor (W_z) at a depth of 20 meters at a specific location. The LPI proposed by (Iwasaki et al., 1981) can be calculated using the following equation.

$$LPI = \int_0^{20} F(z) \times W(z) dz \quad [6]$$

The obtained LPI value is then classified based on Table 2. This index provides an overview of the intensity of liquefaction hazards and helps estimate the potential damage caused by this phenomenon.

Table 2. Liquefaction Potential Index Classification (Sonmez, 2003)

LPI	Liquefaction Potential	Description
0	Very Low	No improvement method is required
$0 < LPI \leq 5$	Low	Investigation required for critical facilities
$5 < LPI \leq 15$	High	improvement and in-depth facility investigation required
$LPI > 15$	Very High	Ground improvement is necessary

RESULTS AND DISCUSSION

Soil Data Processing

In this research, soil data consists of SPT test results and laboratory soil data. This soil data will be processed to obtain the $(N_1)_{60}$ value, then corrected based on Fines Content (FC). As a result, an $(N_1)_{60cs}$ graph is produced for each borehole log point, as shown in Figure 5.

Figure 5 shows the profiles of $(N_1)_{60cs}$ values at depths up to 30 meters at six locations (LP-1 to LP-6). The $(N_1)_{60cs}$ value, obtained from the corrected Standard Penetration Test (SPT), is an essential indicator in determining liquefaction potential. Youd & Idriss (2001) state that if $(N_1)_{60cs} < 30$, it indicates liquefaction potential, as the soil is considered weak and vulnerable to earthquake shaking. In this graph, many $(N_1)_{60cs}$ values are below 30, indicating the potential for liquefaction in some soil layers. Conversely, if the $(N_1)_{60cs}$ value is ≥ 30 , the soil has sufficient density and strength to withstand seismic loading without undergoing significant physical changes. At depths greater than 20 meters, the risk of liquefaction decreases as higher soil pressures help maintain the structure.

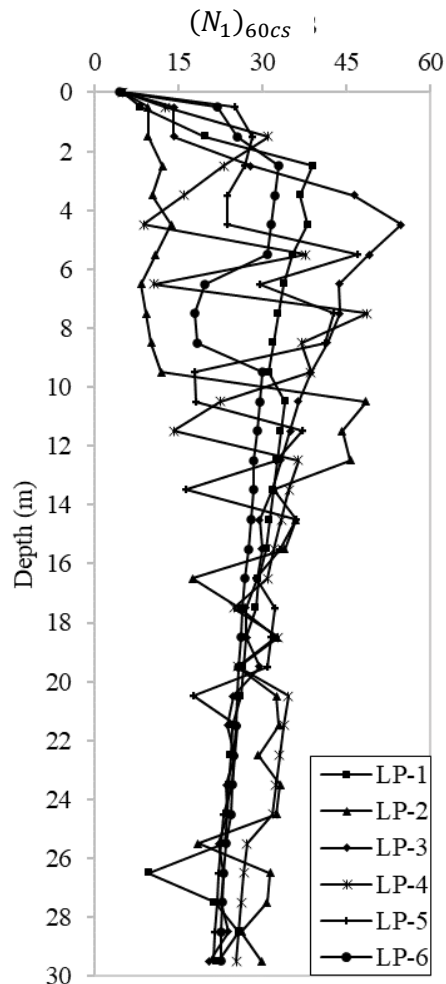


Figure 5. $(N_1)_{60cs}$ graph at each borehole log

DEEPSOIL Analysis

The analysis results in soil profile data showing each soil layer's PGA (Peak Ground Acceleration) value. The PGA values, measured at the base of each soil layer, indicate the maximum ground acceleration during an earthquake and serve as a critical parameter in seismic analysis, as they reflect the level of shaking that structures and infrastructure at the surface will experience. The DEEPSOIL analysis results for each point and depth are displayed in Figure 6.

Figure 6 shows the PGA (Peak Ground Acceleration) profile with depth for six borehole points (LP-1 to LP-6) based on DEEPSOIL analysis. The analysis reveals that amplification occurs at some points, such as LP-1, LP-3, LP-5, and LP-6, indicating increased earthquake shaking intensity due to specific soil layers strengthening seismic waves. Conversely, at points LP-2 and LP-4, deamplification occurs, reflecting a decrease in shaking intensity because the seismic

waves pass through denser or more rigid soil layers, which absorb some of the seismic energy. This analysis helps to understand how soil structure can influence the impact of seismic shaking at the surface.

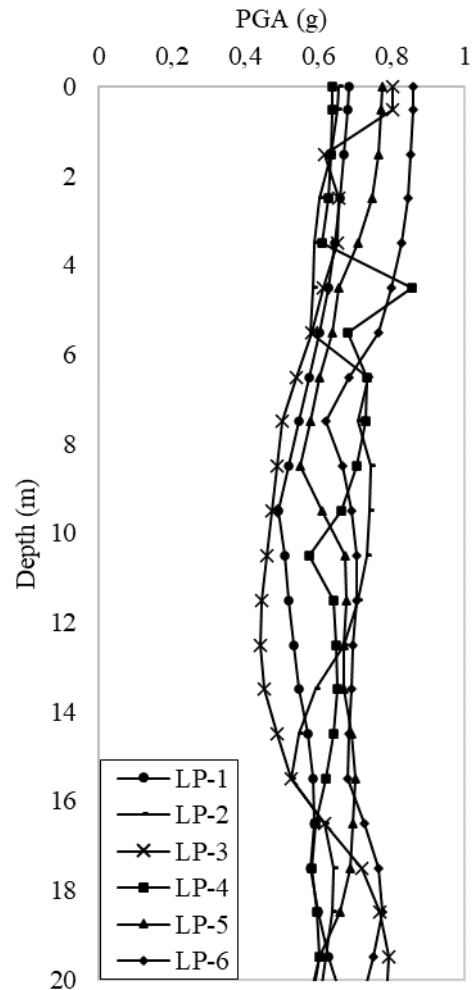


Figure 6. PGA graph at each borehole log

Liquefaction Probability Calculation Results

Liquefaction probability calculations are performed to predict the worst-case probability that liquefaction will occur at a site due to an earthquake or other ground movement. The calculation of liquefaction probability in the methods of Lai et al. (2006) and Juang et al. (2008) is obtained from Equations [4] and [5] with the classification in Table 1. The results of the liquefaction probability calculation are presented in Figures 7 to 18.

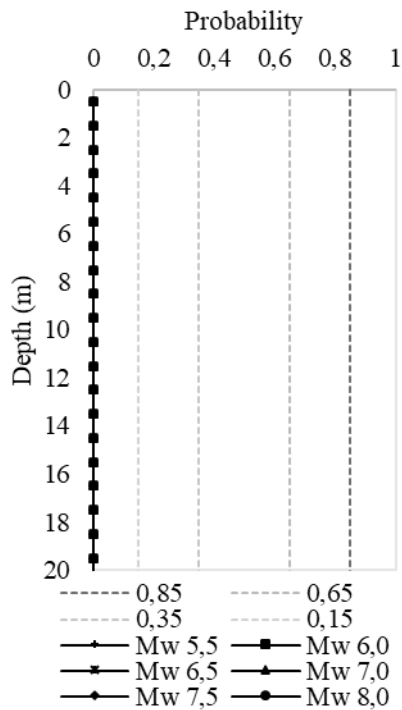


Figure 7. Graph of liquefaction probability analysis results using the Lai et al. (2006) method at point LP-1

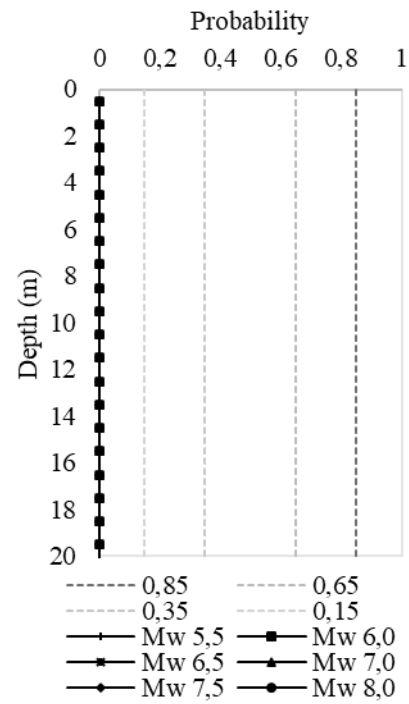


Figure 9. Graph of liquefaction probability analysis results using the Lai et al. (2006) method at point LP-3

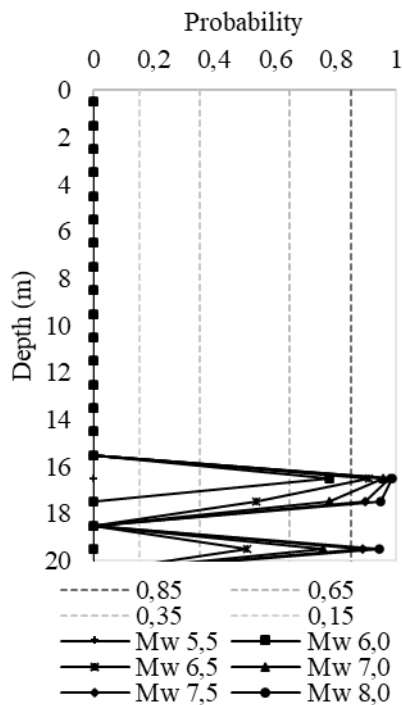


Figure 8. Graph of liquefaction probability analysis results using the Lai et al. (2006) method at point LP-2

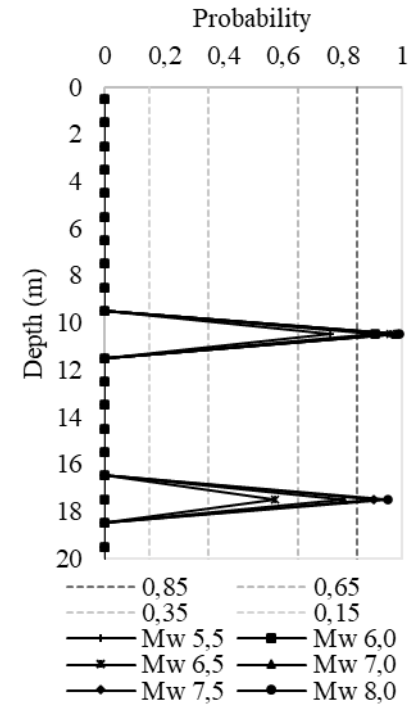


Figure 10. Graph of liquefaction probability analysis results using the Lai et al. (2006) method at point LP-4

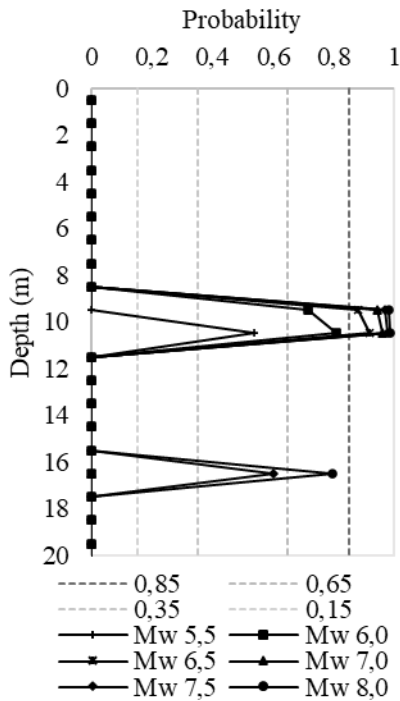


Figure 11. Graph of liquefaction probability analysis results using the Lai et al. (2006) method at point LP-5

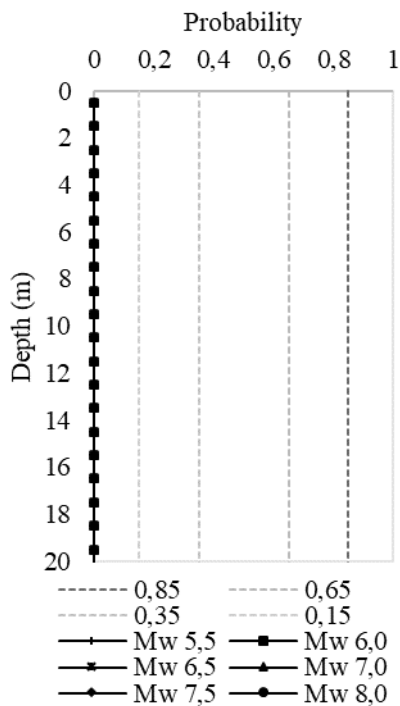


Figure 12. Graph of liquefaction probability analysis results using the Lai et al. (2006) method at point LP-6

Based on the results of the liquefaction probability analysis using the Lai et al. (2006) method for various magnitude (Mw) variations, Figures 7, 9, and 12 indicate no liquefaction potential at the three points,

namely LP-1, LP-3, and LP-6. The liquefaction probability value at these three points is 0, which falls into the “**Almost certainly not liquefied**” category.

Figure 8 shows that point LP-2 has liquefaction potential at depths of 16,5 m to 17,5 m and at 19,5 m, with the most significant probability value occurring at a depth of 16,5 m, where the probability value is 0,99 at Mw 8, falling into the category of “**Almost certainly liquefied**”.

Figure 10 shows that point LP-4 indicates liquefaction potential at depths of 10,5 m and 17,5 m, with the most significant probability value occurring at a depth of 10,5 m, where the probability value is 0,99 at Mw 8 and 7,5, falling into the category of “**Almost certainly liquefied**”.

Figure 11 shows that point LP-5 indicates liquefaction potential at depths of 9,5 m to 10,5 m and at 16,5 m, with the most significant probability value occurring at a depth of 10,5 m, where the probability value is 0,99 at Mw 8, falling into the category of “**Almost certainly liquefied**”.

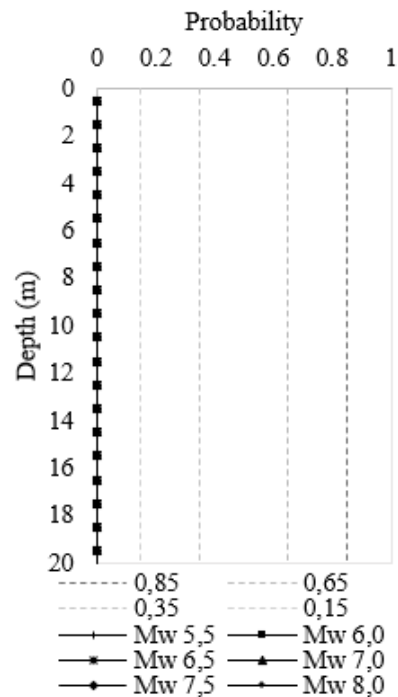


Figure 13. Graph of liquefaction probability analysis results using the Juang et al. (2008) method at point LP-1

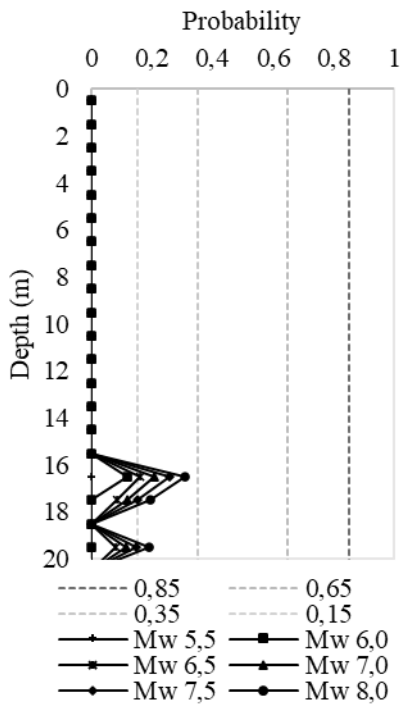


Figure 14. Graph of liquefaction probability analysis results using the Juang et al. (2008) method at point LP-2

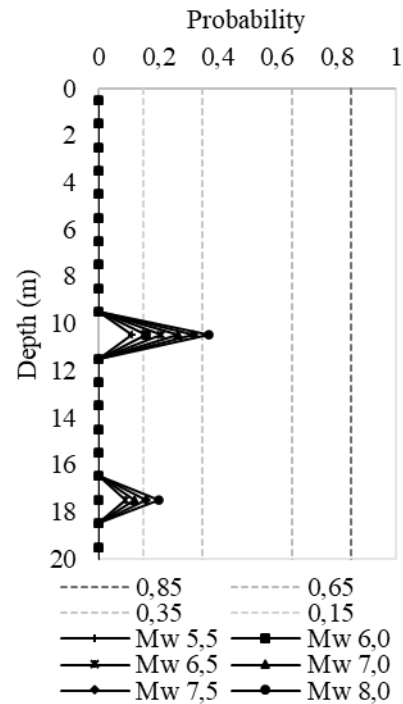


Figure 16. Graph of liquefaction probability analysis results using the Juang et al. (2008) method at point LP-5

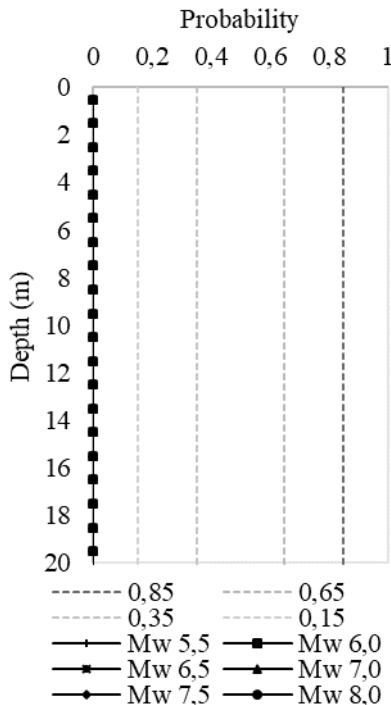


Figure 15. Graph of liquefaction probability analysis results using the Juang et al. (2008) method at point LP-3

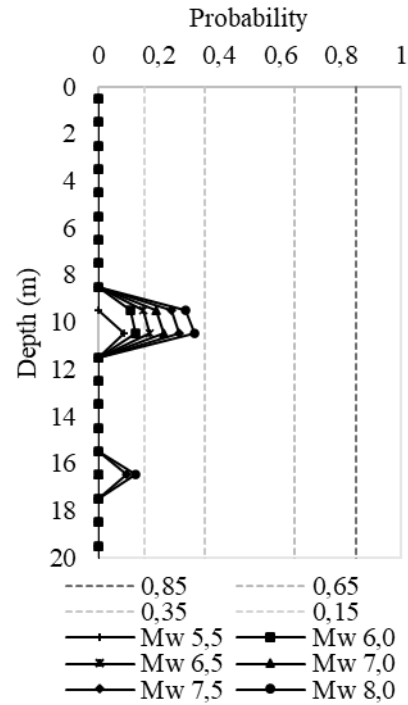


Figure 17. Graph of liquefaction probability analysis results using the Juang et al. (2008) method at point LP-5

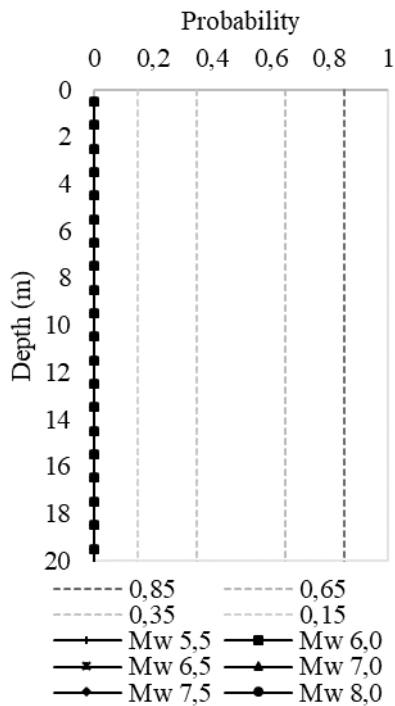


Figure 18. Graph of liquefaction probability analysis results using the Juang et al. (2008) method at point LP-6

Based on the results of the liquefaction probability analysis using the Juang et al. (2008) method for various magnitude (Mw) variations, Figures 13, 15, and 18 indicate no liquefaction potential at the three points, namely LP-1, LP-3, and LP-6. The liquefaction probability value at these three points is 0, which falls into the “**Almost certainly not liquefied**” category.

Figure 14 shows that point LP-2 has liquefaction potential at depths of 16,5 m to 17,5 m and at 19,5 m, with the most significant probability value occurring at a depth of 16,5 m, where the probability value is 0,31 at Mw 8, falling into the category of “**Not likely to be liquefied**”.

Figure 16 shows that point LP-4 indicates liquefaction potential at depths of 10,5 m and 17,5 m, with the most significant probability value occurring at a depth of 10,5 m, where the probability value is 0,37 at Mw 8, falling into the category of “**Not likely to be liquefied**”.

Figure 17 shows that point LP-5 indicates liquefaction potential at depths of 9,5 m to 10,5 m and at 16,5 m, with the most significant probability value occurring at a depth of 10,5 m, where the probability value is 0,32 at Mw 8, falling into the category of “**Not likely to be liquefied**”.

Based on the analysis results using both methods, the outcomes differ, with the Lai et al. (2006) method tending to provide higher probability estimates than the Juang et al. (2008) method.

LPI Calculation Results

The LPI value is calculated from Equation [6] and classified based on Table 2. Based on the calculations, point LP-5 has a high potential for liquefaction with a variation of Mw compared to other points. The results of this calculation are used to evaluate the possibility of liquefaction in an area. The LPI calculation results are presented in Figure 19.

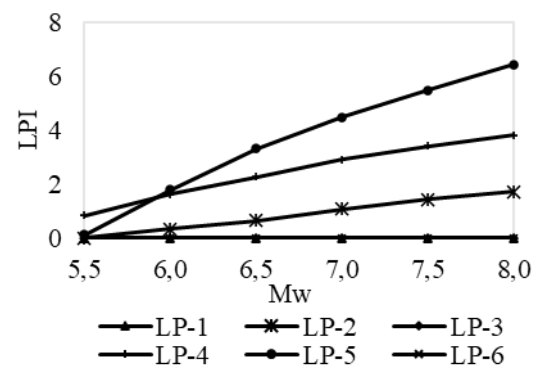


Figure 19. Graph of LPI value analysis results

CONCLUSION

The analysis of liquefaction potential at six soil test points in the Petobo area of Palu City concludes that certain areas exhibit varying degrees of liquefaction potential depending on the earthquake magnitude at each end. LP-5 is the only point with a high level of liquefaction potential, with this category observed for all Mw variations except Mw 5,5. Meanwhile, points LP-1, LP-3, and LP-6 do not show any liquefaction potential.

Increasing earthquake magnitude impacts the probability and LPI values, where a magnitude of 5,5 results in lower values than higher magnitudes. In other words, as the earthquake's magnitude increases, the probability and LPI values obtained from the analysis also increase.

REFERENCE

2022, P. S. G. N. (n.d.). *Disusun oleh : Pusat Studi Gempa Nasional Kerjasama :*

- Chen, C. J., & Juang, C. H. (2000). Calibration of SPT- and CPT-Based Liquefaction Evaluation Methods. *Innovations and Applications in Geotechnical Site Characterization*, 49–64. [https://doi.org/10.1061/40505\(285\)4](https://doi.org/10.1061/40505(285)4)
- Fuady, M., Munadi, R., & Fuady, M. A. K. (2021). Disaster mitigation in Indonesia: between plans and reality. *IOP Conference Series: Materials Science and Engineering*, 1087(1), 12011.
- Hashash, Y. M. A. (2024). *DEEPSOIL Version 7.0*. 1–169.
- Iwasaki, T., Tokida, K., & Tatsuoka, F. (1981). Soil Liquefaction Potential Evaluation with Use of the Simplified Procedure. *International Conferences on Recent Advances in Geotechnical Earthquake Engineering and Soil Dynamics*, 209–214.
- Japan Road Association. (2012). Specifications for Highway Bridges Part II. *Marusan Publishing Division*, September.
- Juang, C. H., Li, D. K., Fang, S. Y., Liu, Z., & Khor, E. H. (2008). Simplified Procedure for Developing Joint Distribution of amax and Mw for Probabilistic Liquefaction Hazard Analysis. *Journal of Geotechnical and Geoenvironmental Engineering*, 134(8), 1050–1058. [https://doi.org/10.1061/\(asce\)1090-0241\(2008\)134:8\(1050\)](https://doi.org/10.1061/(asce)1090-0241(2008)134:8(1050))
- Kramer, S. L. (1996). *Geotechnical Earthquake Engineering*.
- Kumar, D. R., Samui, P., Burman, A., Wipulanusat, W., & Keawsawasvong, S. (2023). Liquefaction susceptibility using machine learning based on SPT data. *Intelligent Systems with Applications*, 20, 200281. <https://doi.org/10.1016/j.iswa.2023.200281>
- Lai, S., Chang, W., & Lin, P. (2006). Logistic Regression Model for Evaluating Soil Liquefaction Probability Using CPT Data. *Journal of Geotechnical and Geoenvironmental Engineering*, June, 694–704.
- Leopatty, H., Alam, R., Efendi, R., Asyhar, L. F., Cholidani, M., Mustarang, A., & Feriansyah, S. (2022). The Identification of Earthquake Shake Levels in Palu City Based on Mw 6,8 Shakemap Scenario by Palu Koro Fault. *Gravitasi*, 21(1). <https://doi.org/10.22487/gravitasi.v21i1.15836>
- Maha Agung, P. A., Sultan, R., Idris, M., Sudjianto, A. T., Ahmad, M. A., & Rouf Hasan, M. F. (2023). Probabilistic of in Situ Seismic Soil Liquefaction Potential Based on CPT-Data in Central Jakarta, Indonesia. *International Journal of Sustainable Construction Engineering and Technology*, 14(1). <https://doi.org/10.30880/ijscet.2023.14.01.021>
- Mase, L. Z. (2018). Studi Keandalan Metode Analisis Likui-faksi Menggunakan SPT Akibat Gempa 8,6 Mw, 12 September 2007 di Area Pesisir Kota Bengkulu. *Jurnal Teknik Sipil*, 25(1), 53. <https://doi.org/10.5614/jts.2018.25.1.7>
- Pamungkas, I. S. I. (2023). *Analisis Potensi Likui-faksi dengan Metode Simplifikasi dan Liquefaction Potential Index di Kota Palu Menggunakan Perhitungan Manual dan Aplikasi UNShake*.
- Poddar, P., Ojha, S., & Gupta, M. K. (2023). Probabilistic and deterministic-based approach for liquefaction potential assessment of layered soil. *Natural Hazards*, 118(2), 993–1012. <https://doi.org/10.1007/s11069-023-06031-9>
- Rahman, M. A., Fathani, T. F., Rifa'i, A., & Hidayat, M. S. (2020). *Analisis Tingkat Potensi Likui-faksi di Kawasan Underpass Yogyakarta International Airport*. 16(2), 91–104.
- Reddy, N. D. K., Gupta, A. K., & Sahu, A. K. (2024). Assessment of Soil Liquefaction Potential Using Genetic Programming Using a Probability-Based Approach. *Iranian Journal of Science and Technology, Transactions of Civil Engineering*. <https://doi.org/10.1007/s40996-024-01421-w>
- Sonmez, H. (2003). Modification of the liquefaction potential index and liquefaction susceptibility mapping for a liquefaction-prone area (Inegol, Turkey). *Environmental Geology*, 44(7), 862–871. <https://doi.org/10.1007/s00254-003-0831-0>
- Tijow, K. C., Sompie, O. B. A., & Ticoh, J. H. (2018). Analisis Potensi Likui-faksi Tanah Berdasarkan Data Standart

Penetration Test (Spt) Studi Kasus :
Dermaga Bitung, Sulawesi Utara. *Jurnal
Sipil Statik*, 6(7), 491–500.

Youd, B. T. L., & Idriss, I. M. (2001).
Liquefaction Resistance of Soils :
Summary Report From the 1996
NNEER and 1998 NCEER/ NSF
Workshops on Evaluation of
LiquefactionResistance of Soils. *Journal
of Geotechnical and Geoenvironmental
Engineering*, 127(10), 817–833.